



ORIGINAL ARTICLE

Tensile strength of ostrich carotid artery decellularized with liquefied dimethyl ether and DNase: An effort in addressing religious and cultural concerns



Hideki Kanda ^{a,*}, Kento Oya ^a, Toshihira Irisawa ^b, Wahyudiono ^{a,c},
Motonobu Goto ^{a,d}

^a Department of Materials Process Engineering, Nagoya University, Nagoya 464-8603, Japan

^b Department of Chemical Systems Engineering, Nagoya University, Nagoya 464-8603, Japan

^c New Industry Creation Hatchery Center, Tohoku University, 6-6-10 Aoba, Aramaki, Aoba-ku, Sendai 980-8579, Japan

^d Super Critical Technology Centre Co. Ltd., Kuwana, Mie 511-0838, Japan

Received 5 September 2022; accepted 10 January 2023

Available online 16 January 2023

KEYWORDS

Decellularization;
Scaffold;
Subcritical extraction;
Liquefied gas;
Mechanical properties

Abstract In a previous report, we proposed a method for decellularizing ostrich carotid arteries by removing lipids from the arteries using liquefied dimethyl ether (DME) instead of the conventional sodium dodecyl sulfate (SDS). This is followed by DNA fragmentation with DNase. In the present study, the physical properties of ostrich carotid arteries decellularized using the DME method were evaluated via tensile tests. Results showed that the tissue with SDS broke under less than half the stress of the original ostrich carotid artery. In contrast, the tissue treated with liquefied DME withstood the same level of the original tissue. Both decellularized tissues by liquefied DME showed flexibility comparable to that of the original tissue. We attributed this to the no C=N bonds temporarily generated by dehydration through the Schiff-base reaction when lipids were removed by liquefied DME.

© 2023 The Author(s). Published by Elsevier B.V. on behalf of King Saud University. This is an open access article under the CC BY license (<http://creativecommons.org/licenses/by/4.0/>).

1. Introduction

At the University of Maryland Medical Center in the USA, a genetically engineered, rejection-suppressed pig heart was transplanted into a human on 7 January 2022 due to a lack of donors (Shah et al., 2022). However, there are problems with interspecies organ transplantation, such as organ rejection and the transmission of emerging new viruses through interspecies transplantation (Wadiwala et al., 2022). The patient with the transplanted pig heart died on 9 March 2022 (Wang et al., 2022), and xenotransplantation is still a developing tech-

* Corresponding author.

E-mail address: kanda.hideki@material.nagoya-u.ac.jp (H. Kanda).

Peer review under responsibility of King Saud University.



nology. In addition, the transplantation of pig hearts into humans leaves a serious problem: the life span of pigs is shorter than that of humans. To solve these problems, researchers in regenerative medicine are attempting to create tissues and organs from the patient's pluripotent cells, but three-dimensional (3D) culturing is difficult and requires 3D scaffold materials. Before the scaffold is transplanted into a human, the patient's own cells are cultured in the 3D scaffold. The patient's cells secrete substances that make up the extracellular matrix, and the scaffold itself is replaced with substances derived from the patient's cells. Without scaffold materials, the pluripotent cells grow in a flat shape on a petri dish. Clinical trials using flat tissues such as the retina (Mandai et al., 2017) and myocardium (Miyagawa et al., 2022) have progressed, but little progress has been made in 3D tissues. This suggests that the creation of scaffold materials is not a sufficient technique, as the extracellular matrix is created by the removal of genetic information from animal tissues, i.e., decellularization. Pig tissue is frequently used (White et al., 2005; Korossis et al., 2005; Gilbert et al., 2006; Prasertsung et al., 2008; Rosario et al., 2008; Funamoto et al., 2010; Flynn, 2010; Kajbafzadeh et al., 2014; Wolinsky and Glagov, 1964; Hashimoto et al., 2010; Moffat et al., 2022; Xing et al., 2015; Kanda et al., 2021a) because it can grow to the size of a human tissue in a few months and the structure and function of the pig heart are similar to those of the human heart (Wadiwala et al., 2022). For these reasons, interspecies heart transplants have been performed, as mentioned at the beginning of this section. However, pigs are viewed unfavorably in some religions and cultures, and many people have a strong psychological aversion to pig-derived tissue being incorporated as part of their bodies. Few studies have been performed on the decellularization of non-pig tissues. Examples include the decellularization of ostrich tendons (Hosseini et al., 2015), ostrich carotid arteries (Kanda et al., 2021b), and the bovine pericardium (Mendoza-Novelo et al., 2011).

In summary, the problems can be summarized as follows: the lack of donors, which necessitates interspecies organ transplants; the immaturity of the technology for creating extracellular matrices for 3D cultures; and the use of pig tissue.

The simplest and most common method of decellularization is the removal of genetic information using sodium dodecyl sulfate (SDS) and DNase (White et al., 2005; Korossis et al., 2005; Gilbert et al., 2006; Prasertsung et al., 2008; Rosario et al., 2008; Funamoto et al., 2010; Flynn, 2010; Kajbafzadeh et al., 2014; Wolinsky and Glagov, 1964; Hashimoto et al., 2010; Moffat et al., 2022; Xing et al., 2015). SDS is a strong surfactant and can thoroughly remove lipids from tissue. However, it must be sufficiently removed from decellularized tissues, as it causes inflammation, which is why people experience skin irritation caused by dishwashing. In addition, fibronectin, glycosaminoglycans, proteoglycans, extracellular matrix regulators, and secreted factors are easily lost during decellularization with SDS (Moffat et al., 2022).

Although bases and acids are highly reactive and easy to use, their high reactivity causes damage to biological tissue. Procedures for decellularization using bases and acids include alkaline swelling and peracetic acid treatment (Gilpin and Yang, 2017). Thin tissues such as bladder tissue (Gilbert et al., 2008) and the small intestinal submucosa (Syed et al., 2014) were decellularized with peracetic acid and found to be biocompatible, but the decellularization was incomplete (Syed et al., 2014). Furthermore, the mechanical properties of these decellularized tissues were altered, with increases in the yield stress and elastic modulus (Gilbert et al., 2008). Thus, the desired elasticity was not achieved, owing to the hardening of the extracellular matrix. Protocols using alkaline solutions and mixtures with surfactants have been applied to the bovine pericardium (Mendoza-Novelo et al., 2011) and porcine carotid arteries (Chuang et al., 2009). However, decellularized tissue swelling due to collagen being negatively charged in the tissue has been reported, and even after this swelling was reversed with ammonium sulphate, the glycosaminoglycan content and viscoelasticity of the tissue were reduced (Mendoza-Novelo et al., 2011).

For decellularized tissue to play a major role in regenerative medicine, its basic strength properties must be understood. In a previous study, we investigated the use of liquefied dimethyl ether (DME) instead of an aqueous SDS solution as a medium to decellularize a porcine aorta (Kanda et al., 2021a) and an ostrich carotid artery (Kanda et al., 2021b). In the DME treatment, highly volatile DME is used to disrupt the cell membrane and remove cellular lipids. The treatment involves three steps, as described in Section 2. Briefly, lipids are first extracted from the samples using liquefied DME under pressure for 1 h. The lipid-removed samples are then fragmented with DNA using a DNase solution for 3–5 d. Finally, the samples are washed with water and ethanol to remove DNA fragments. This procedure is identical to the conventional SDS method except that liquefied DME is used instead of SDS.

An important advantage of DME is its safety. Although DME is the simplest ether, it has different properties from the well-known ethers, such as ethyl ether. DME is not toxic to microorganisms (Kanda et al., 2021a); thus, the European Food Safety Authority (EFSA) has recognized it as a food-processing medium (Panel on Food Contact Materials, Enzymes, Flavourings and Processing Aids, 2015). Additionally, because of its low boiling point of $-24.8\text{ }^{\circ}\text{C}$ (Wu et al., 2011), it is liquefied when used as a solvent and does not remain in the tissue from which lipids are removed (Kanda et al., 2021a; 2021b). DME also can extract the all lipids from microalgae and biosolids; thus, it is often used as a solvent for total lipid determination (Li et al., 2014; Kanda et al., 2015; Oshita et al., 2015).

However, DME can form weak hydrogen bonds (Tatamitani et al., 2002) and is partially mixed with water in a liquefied state (Holldorff and Knapp 1988; Tallon and Fenton 2010). Therefore, in addition to lipids, water is extracted from animal tissues, resulting in dry tissues (Kanda et al., 2021a; 2021b). In the porcine aorta, the removal of lipids and water with liquefied DME causes a Schiff-base reaction of dehydration in the collagen, during which C=N bonds are formed between neighboring collagen fibers. These bonds are subsequently eliminated by treatment with a DNase solution, and the Fourier transform infrared (FT-IR) spectrum is similar to that of the original porcine aorta (Kanda et al., 2021a). The formation of temporary C=N bonds increases the tensile strength of the decellularized tissue of the porcine aorta compared with the original porcine aorta but reduces its flexibility (Kanda et al., 2022). In contrast, in the case of ostrich carotid arteries, FT-IR measurements have indicated that C=N bonds are not formed, even after the removal of lipids and water using liquefied DME (Kanda et al., 2021b). These findings suggest that decellularized tissue created from ostrich carotid arteries may have better mechanical properties than decellularized tissue created from porcine aortas.

Therefore, in this study, we measured the tensile strengths of two decellularized ostrich carotid arteries—one prepared with conventional SDS and DNase treatment and another prepared with liquefied DME and DNase treatment—to evaluate the ease of fracture and deformation of the decellularized tissues.

2. Materials and methods

2.1. Materials

The ostrich carotid artery samples used in this study were purchased from a meat supplier (Oyama Ostrich Farm, Oyama, Japan) and were taken from ostriches slaughtered for meat processing. Therefore, ostriches were not slaughtered specifically for this experiment. First, excess lipid adhering to the ostrich carotid artery was scraped off with a knife. Then, the ostrich carotid artery was cut into 5.5-cm-long pieces, which were stored in phosphate-buffered saline at $4\text{ }^{\circ}\text{C}$. The moisture content of the ostrich carotid artery (36–39 wt%) was confirmed by measuring the weight loss of the artery when it was heated to $107\text{ }^{\circ}\text{C}$. Liquefied DME in spray cans (Spray

Work Air Can 420D) was purchased from Tamiya (Shizuoka, Japan) and used without further purification.

2.2. Decellularization using SDS or DME

In the previous report (Kanda et al., 2021b), using the proposed method, ostrich carotid arteries were successfully decellularized with liquefied DME and DNase, and the following three criteria for successful decellularization were satisfied. The properties of decellularized ostrich carotid arteries have been described in the previous report. 1) no cell nuclei were observed in a microscopic examination of the haematoxylin-eosin-stained decellularized tissue, 2) the residual DNA content in the decellularized tissue was < 50 ng/mg-dry, and 3) the content of residual DNA fragments in the decellularized tissue was < 200 bp (Rana et al., 2017; Crapo et al., 2011).

In the present study, the ostrich carotid artery was decellularized using the same protocol as in the previous report. The decellularization protocol involved three steps: 1) removal of lipids from the ostrich carotid arteries using liquefied DME or SDS, 2) fragmentation of DNA via DNase treatment, and 3) washing to remove the SDS and fragmented DNA. The only difference between the liquefied DME and SDS treatments was the first step.

2.2.1. Liquefied DME treatment

Liquefied DME treatment was performed according to the protocol used in a previous study on decellularization (Kanda et al., 2021b). Briefly, a cylindrical column was filled with the ostrich carotid artery samples, and liquefied DME was fed to the column at 10 ± 1 mL/min for 1 h. Following the DME treatment, the inside of the column was depressurized to evaporate the internal DME, and the ostrich carotid arteries were removed. The ostrich carotid arteries were then shaken in a 0.2 % DNase solution (Roche Diagnostic, Tokyo, Japan) at 4 °C for 7 d. This period exceeded the 5-d condition required to meet the criteria in the previous study (Kanda et al., 2021b), for ensuring successful decellularization. Following the DNase treatment, the ostrich carotid arteries were washed with 80/20 (v/v) ethanol/phosphate-buffered saline for 3 d. Ethanol was purchased from FujiFilm Wako Pure Chemical Corporation, Osaka, Japan. The phosphate-buffered saline (PBS, pH 7.4, Gibco 10010023, Thermo Fisher Scientific K.K., Tokyo, Japan) was prepared with penicillin-streptomycin solution (FujiFilm Wako Pure Chemical Corporation) added to achieve a 1 % concentration.

2.2.2. SDS treatment

SDS decellularization was performed using a previous study on decellularization (Korossis et al., 2005). Briefly, the ostrich carotid arteries were washed with 10 mM tris-(hydroxymethyl)-aminomethane buffer (Nippon Gene Co., Ltd., Tokyo, Japan) with 0.1 % ethylenediaminetetraacetic acid (Nippon Gene Co., Ltd.) and 0.1 % SDS (FujiFilm Wako Pure Chemical Corporation) for 24 h at room temperature and then rinsed thrice with the phosphate-buffered saline. The decellularized tissues were then obtained via treatment with the DNase solution and washing, similar to the DME treatment.

2.3. Tensile-strength measurement

The tensile strengths of the original ostrich carotid arteries and decellularized samples were measured using a previously reported method (Wu et al., 2015). Both ends of the samples were clamped in a load displacement transducer (SL-6001; Imada Seisakusho, Toyohashi, Japan), as shown in Fig. 1. The samples were cut open longitudinally as a rectangular shape 5.5 cm long and 1.5 cm wide. Each sample was strained at a rate of 5 mm/min longitudinally. Seven measurements were performed, and the lowest and highest tensile strengths were rejected. The stress curves obtained from the remaining five tests were averaged.

3. Results and discussion

Fig. 2 shows the decellularized tissues obtained using DME and SDS. The SDS-treated tissue was approximately 6.5 cm long and 1.8 cm wide, and expanded 18–20 % in length and width compared to the original tissue. In contrast, the DME-treated tissue shrank to approximately 5.2 cm in length, 5 % from its original tissue. The widths changed so little that no significant differences could be measured. This is similar to the size changes observed in porcine aorta decellularised with SDS and DME in a previous study (Kanda et al., 2021a.) This was consistent with of haematoxylin-eosin staining results from previous studies: decellularized porcine aorta and ostrich carotid artery tissue obtained using DME was densely packed

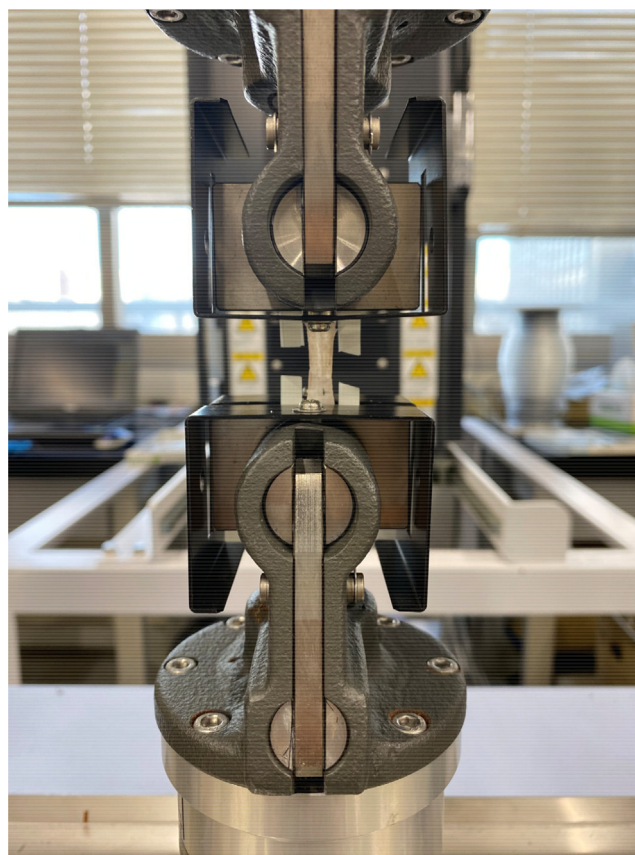


Fig. 1 Decellularized ostrich carotid artery set on the load displacement transducer.

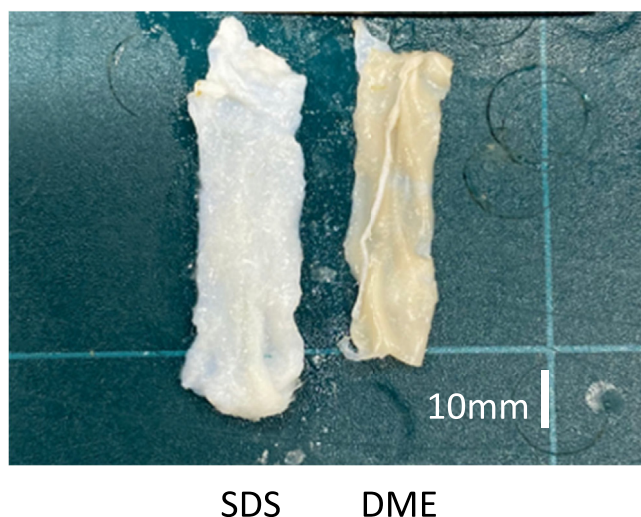


Fig. 2 Photographs of ostrich carotid artery samples after decellularization and before.

with protein fibers (Kanda et al., 2021a and 2021b), whereas large gaps between protein fibers appeared in porcine aorta tissue decellularized with SDS (Funamoto et al., 2010). In previous studies, arteries had a three-layer (outer, middle, and inner) structure. The outer layer (also known as the adventitia) is surrounded by loose connective tissue consisting mainly of thick bundles of helically arranged collagen fibers. The middle layer (media) consists of smooth muscle cells, a network of elastic and collagen fibers, and elastic lamellae separating the media into circumferentially isotropic fiber-reinforcing units. The inner layer (intima) consists mainly of a single layer of endothelial cells, thin basement membrane, and subendothelial layer of collagen fibers (Tsamis et al., 2013; Gasser et al., 2006). Studies have indicated that the direction of the fibers is closer to the axial direction in the adventitia, closer to the circumferential direction in the media, and somewhere between these two directions in the intima (Schriebl et al., 2012). Thus, no significant anisotropy is observed in the fibers that comprise the vessels, and the isotropic expansion in the three directions is consistent with the structure.

Fig. 3 shows the results for the samples cut along the longitudinal direction. The decellularized tissue treated with liquefied

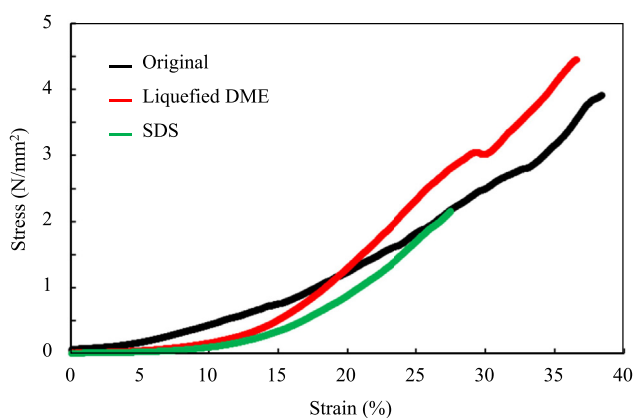


Fig. 3 Average strain–stress curves of the ostrich carotid artery samples. “Original” refers to the ostrich carotid artery prior to decellularization.

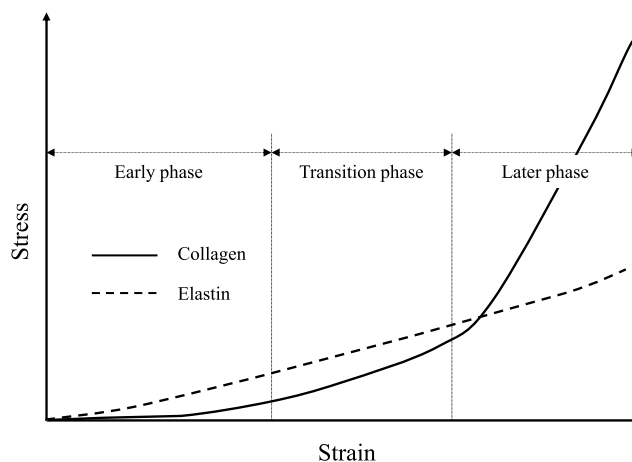


Fig. 4 Stress-response properties of collagen and elastin when elongated.

DME exhibited almost the same degree of elongation as the original ostrich carotid artery under the same stresses; i.e., it did not exhibit atherosclerotic-like variations, which are observed in porcine aortas. This suggests that the DME treatment did not cause a Schiff-base reaction in the ostrich carotid arteries, as intended (see Section 1), and that the flexibility of the collagen was not compromised as a result. The SDS-treated tissues exhibited a similar stress response to the original samples and the samples decellularized with liquefied DME until midway through tensile test, but they broke easily at half the maximum stress withstood by the DME-treated samples. This was consistent with previous findings indicating that decellularization with SDS altered the tissue microstructure and compromised the biomechanical integrity of the extracellular matrix in exchange for a strong exfoliating effect (Xu et al., 2014).

A previous study indicated that arterial tissue is mainly composed of collagen and elastin and that tensile stress is applied to elastin in the early stages of tension and to collagen in the late stages of tension (Wu, et al., 2015), as shown in Fig. 4. The ostrich carotid arteries decellularized with SDS responded to tensile stress similarly to the original arteries and those decellularized with liquefied DME until halfway through the tensile test. This breakage suggests that elastin was not significantly damaged by SDS, but the collagen was.

Thus, unlike the porcine aorta, the ostrich carotid artery, when decellularized with liquefied DME and DNase, does not change its strength and flexibility from the original tissue, indicating that the ostrich carotid artery is an extremely mechanically superior scaffold material. Not only that, but ostrich carotid has the potential to provide decellularized tissue for people with religious and cultural concerns about pigs, such as Muslims, who make up 1/4 of the world population.

4. Conclusions

Tensile tests were performed on decellularized tissue obtained from ostrich carotid artery by lipid removal with liquefied DME and DNA fragmentation with DNase. Results showed that the tissue with SDS broke under less than half the stress of the original ostrich carotid artery. In contrast, the tissue treated with liquefied DME withstood the same level of the original tissue. Both decellularized tissues by SDS and liquefied DME showed flexibility comparable to that of the original tis-

sue. We attributed this to the no C=N bonds temporarily generated by dehydration through the Schiff-base reaction when lipids were removed by SDS or liquefied DME. Ostrich carotid artery is an extremely mechanically superior scaffold material than porcine aorta. Ostrich carotid artery also has the potential to provide decellularized tissue for those with religious and cultural considerations for pigs.

Funding

The authors disclose receipt of financial support from the following organizations for the research, authorship, and/or publication of this article: the Japan Society for the Promotion of Science (Grant No 17K06922 and JP20K05192), the Foundation of Public Interest of Tatematsu (Kariya, Japan), and the Ito Foundation (Tokyo, Japan).

CRedit authorship contribution statement

Hideki Kanda: Conceptualization, Methodology, Investigation, Writing – original draft, Writing – review & editing, Project administration, Resources, Funding acquisition. **Kento Oya:** Investigation, Data curation, Visualization. **Toshihira Irisawa:** Methodology, Resources. **Wahyudiono:** Supervision. **Motonobu Goto:** Supervision.

Declaration of Competing Interest

The authors declare that they have no known competing financial interests or personal relationships that could have appeared to influence the work reported in this paper.

References

- Chuang, T.-H., Stabler, C., Simionescu, A., Simionescu, D.T., 2009. Polyphenol-stabilized tubular elastin scaffolds for tissue engineered vascular grafts. *Tissue Eng. Part A* 15, 2837–2851. <https://doi.org/10.1089/ten.tea.2008.0394>.
- Crapo, P.M., Gilbert, T.W., Badylak, S.F., 2011. An overview of tissue and whole organ decellularization processes. *Biomaterials* 32, 3233–3243. <https://doi.org/10.1016/j.biomaterials.2011.01.057>.
- Flynn, L.E., 2010. The use of decellularized adipose tissue to provide an inductive microenvironment for the adipogenic differentiation of human adiposederived stem cells. *Biomaterials* 31, 4715–4724. <https://doi.org/10.1016/j.biomaterials.2010.02.046>.
- Funamoto, S., Nam, K., Kimura, T., Murakoshi, A., Hashimoto, Y., Niwaya, K., Kitamura, S., Fujisato, T., Kishida, A., 2010. The use of high-hydrostatic pressure treatment to decellularize blood vessels. *Biomaterials* 31, 3590–3595. <https://doi.org/10.1016/j.biomaterials.2010.01.073>.
- Gasser, T.C., Ogden, R.W., Holzapfel, G.A., 2006. Hyperelastic modelling of arterial layers with distributed collagen fibre orientations. *J. R. Soc. Interface* 3, 15–35. <https://doi.org/10.1098/rsif.2005.0073>.
- Gilbert, T.W., Sellaro, T.L., Badylak, S.F., 2006. Decellularization of tissues and organs. *Biomaterials* 27, 3675–3683. <https://doi.org/10.1016/j.biomaterials.2006.02.014>.
- Gilbert, T.W., Wognum, S., Joyce, E.M., Freytes, D.O., Sacks, M.S., Badylak, S.F., 2008. Collagen fiber alignment and biaxial mechanical behavior of porcine urinary bladder derived extracellular matrix. *Biomaterials* 29, 4775–4782. <https://doi.org/10.1016/j.biomaterials.2008.08.022>.
- Gilpin, A., Yang, Y., 2017. Decellularization strategies for regenerative medicine: from processing techniques to applications. *BioMed Res. Int.* 2017, 9831534. <https://doi.org/10.1155/2017/9831534>.
- Hashimoto, Y., Funamoto, S., Sasaki, S., Honda, T., Hattori, S., Nam, K., Kimura, T., Mochizuki, M., Fujisato, T., Kobayashi, H., Kishida, A., 2010. Preparation and characterization of decellularized cornea using high hydrostatic pressurization for corneal tissue engineering. *Biomaterials* 31, 3941–3948. <https://doi.org/10.1016/j.biomaterials.2010.01.122>.
- Holldorff, H., Knapp, H., 1988. Binary vapor-liquid-liquid equilibrium of dimethyl ether-water and mutual solubilities of methyl chloride and water: experimental results and data reduction. *Fluid Phase Equilib.* 44, 195–209. [https://doi.org/10.1016/0378-3812\(88\)80111-0](https://doi.org/10.1016/0378-3812(88)80111-0).
- Hosseini, S., Hasanzadeh, S., Shahrooz, R., 2015. Tissue engineering and histology of ostrich tendon. *Int. J. Biol. Pharm. Allied Sci.* 4, 232–241.
- Kajbafzadeh, A.M., Sabetkish, S., Heidari, R., Ebadi, M., 2014. Tissue-engineered cholecyst-derived extracellular matrix: a biomaterial for in vivo autologous bladder muscular wall regeneration. *Pediatr. Surg. Int.* 30, 371–380. <https://doi.org/10.1007/s00383-014-3474-1>.
- Kanda, H., Ando, D., Hoshino, R., Yamamoto, T., Wahyudiono, Suzuki, S., Shinohara, S., Goto, M., 2021a. Surfactant-free decellularization of porcine aortic tissue by subcritical dimethyl ether. *ACS Omega* 6, 13417–13425. <https://doi.org/10.1021/acsomega.1c01549>.
- Kanda, H., Ando, D., Oya, K., Wahyudiono, Goto, M., 2021b. Surfactant-free preparation of an ostrich carotid artery scaffold using liquefied dimethyl ether and DNase. *Arab. J. Chem.* 14, 103280. <https://doi.org/10.1016/j.arabj.2021.103280>.
- Kanda, H., Oya, K., Irisawa, T., Wahyudiono, Goto, M., 2022. Tensile strength of porcine aortas decellularized with liquefied dimethyl ether and DNase. in press, *ACS Omega* 7, 34449–34453. <https://doi.org/10.1021/acsomega.2c04103>.
- Kanda, H., Li, P., Goto, M., Makino, H., 2015. Energy-saving lipid extraction from wet *Euglena gracilis* by the low-boiling-point solvent dimethyl ether. *Energies* 8, 610–620. <https://doi.org/10.3390/en8010610>.
- Korossis, S.A., Wilcox, H.E., Watterson, K.G., Kearney, J.N., Ingham, E., Fisher, J., 2005. In-vitro assessment of the functional performance of the decellularized intact porcine aortic root. *J. Heart Valve Dis.* 14, 408–421.
- Li, P., Kanda, H., Makino, H., 2014. Simultaneous production of bio-solid fuel and bio-crude from vegetal biomass using liquefied dimethyl ether. *Fuel* 116, 370–376. <https://doi.org/10.1016/j.fuel.2013.08.020>.
- Mandai, M., Watanabe, A., Kurimoto, Y., Hirami, Y., Morinaga, C., Daimon, T., Fujihara, M., Akimaru, H., Sakai, N., Shibata, Y., Terada, M., Nomiya, Y., Tanishima, S., Nakamura, M., Kamao, H., Sugita, S., Onishi, A., Ito, T., Fujita, K., Kawamata, S., Go, M. J., Shinohara, C., Hata, K., Sawada, M., Yamamoto, M., Ohta, S., Ohara, Y., Yoshida, K., Kuwahara, J., Kitano, Y., Amano, N., Umekage, M., Kitaoka, F., Tanaka, A., Okada, C., Takasu, N., Ogawa, S., Yamanaka, S., Takahashi, M., 2017. Autologous induced stem-cell-derived retinal cells for macular degeneration. *N. Engl. J. Med.* 376, 1038–1046. <https://doi.org/10.1056/NEJMoa1608368>.
- Mendoza-Novelo, B., Avila, E.E., Cauich-Rodríguez, J.V., Jorge-Herrero, E., Rojo, F.J., Guinea, G.V., Mata-Mata, J.L., 2011. Decellularization of pericardial tissue and its impact on tensile viscoelasticity and glycosaminoglycan content. *Acta Biomater.* 7, 1241–1248. <https://doi.org/10.1016/j.actbio.2010.11.017>.
- Miyagawa, S., Kainuma, S., Kawamura, T., Suzuki, K., Ito, Y., Iseoka, H., Ito, E., Takeda, M., Sasai, M., Mochizuki-Oda, N., Shimamoto, T., Nitta, Y., Dohi, H., Watabe, T., Sakata, Y., Toda, K., Sawa, Y., 2022. Case report: Transplantation of iPSC-derived cardiomyocyte patches for ischemic cardiomyopathy. *Front. Cardiovasc. Med.* 9. <https://doi.org/10.3389/fcvm.2022.950829>

- Moffat, D., Ye, K., Jin, S., 2022. Decellularization for the retention of tissue niches. *J. Tissue Eng.* <https://doi.org/10.1177/20417314221101151>.
- Oshita, K., Toda, S., Takaoka, M., Kanda, H., Fujimori, T., Matsukawa, K., Fujiwara, T., 2015. Solid fuel production from cattle manure by dewatering using liquefied dimethyl ether. *Fuel* 159, 7–14. <https://doi.org/10.1016/j.fuel.2015.06.063>.
- Panel on Food Contact Materials, Enzymes, Flavourings and Processing Aids. 2015. Scientific opinion on the safety of use of dimethyl ether as an extraction solvent under the intended conditions of use and the proposed maximum residual limits. *EFSA J.* 13, 4174. <https://doi.org/10.2903/j.efsa.2015.4174>
- Prasertung, I., Kanokpanont, S., Bunaprasert, T., Thanakit, V., Damrongsakkul, S., 2008. Development of acellular dermis from porcine skin using periodic pressurized technique. *J. Biomed. Mater. Res. Part B Appl. Biomater.* 85B, 210–219. <https://doi.org/10.1002/jbm.b.30938>.
- Rana, D., Zreiqat, H., Benkirane-Hessel, N., Ramakrishna, S., Ramalingam, M., 2017. Development of decellularized scaffolds for stem cell-driven tissue engineering. *J. Tissue Eng. Regen. Med.* 11, 942–965. <https://doi.org/10.1002/term.2061>.
- Rosario, D.J., Reilly, G.C., Salah, E.A., Glover, M., Bullock, A.J., Macneil, S., 2008. Decellularization and sterilization of porcine urinary bladder matrix for tissue engineering in the lower urinary tract. *Regen. Med.* 3, 145–156. <https://doi.org/10.2217/17460751.3.2.145>.
- Schriebl, A.J., Zeindlinger, G., Pierce, D.M., Regitnig, P., Holzapfel, G.A., 2012. Determination of the layer-specific distributed collagen fibre orientations in human thoracic and abdominal aortas and common iliac arteries. *J. R. Soc. Interface* 9, 1275–1286. <https://doi.org/10.1098/rsif.2011.0727>.
- Shah, A., Goerlich, C.E., Pasrija, C., Hirsch, J., Fisher, S., Odonkor, P., Strauss, E., Ayares, D., Mohiuddin, M.M., Griffith, B.P., 2022. Anatomical differences between human and pig hearts and its relevance for cardiac xenotransplantation surgical technique. *JACC: Case Reports* 4, 1049–1052. <https://doi.org/10.1016/j.jaccas.2022.06.011>.
- Syed, O., Walters, N.J., Day, R.M., Kim, H.-W., Knowles, J.C., 2014. Evaluation of decellularization protocols for production of tubular small intestine submucosa scaffolds for use in oesophageal tissue engineering. *Acta Biomater.* 10, 5043–5054. <https://doi.org/10.1016/j.actbio.2014.08.024>.
- Tallon, S., Fenton, K., 2010. The solubility of water in mixtures of dimethyl ether and carbon dioxide. *Fluid Phase Equilib.* 298, 60–66. <https://doi.org/10.1016/j.fluid.2010.07.009>.
- Tatamitani, Y., Liu, B., Shimada, J., Ogata, T., Ottaviani, P., Maris, A., Caminati, W., Alonso, J.L., 2002. Weak, improper, C–O…H–C hydrogen bonds in the dimethyl ether dimer. *J. Am. Chem. Soc.* 124, 2739–2743. <https://doi.org/10.1021/ja0164069>.
- Tsamis, A., Krawiec, J.T., Vorp, D.A., 2013. Elastin and collagen fibre microstructure of the human aorta in ageing and disease: a review. *J. R. Soc. Interface* 10 (83), 20121004. <https://doi.org/10.1098/rsif.2012.1004>.
- Wadiwala, I.J., Garg, P., Yazji, J.H., Alamouti-fard, E., Alomari, M., Hussain, M.W.A., Elawady, M.S., Jacob, S., 2022. Evolution of xenotransplantation as an alternative to shortage of donors in heart transplantation. *Cureus* 14 (6), e26284.
- Wang, W., He, W., Ruan, Y., Geng, Q., 2022. First pig-to-human heart transplantation. *Innovation* 3, <https://doi.org/10.1016/j.xinn.2022.100223>.
- White, J.K., Agnihotri, A.K., Titus, J.S., Torchiana, D.F., 2005. A stentless trileaflet valve from a sheet of decellularized porcine small intestinal submucosa. *Ann. Thorac. Surg.* 80, 704–707. <https://doi.org/10.1016/j.athoracsur.2004.08.063>.
- Wolinsky, H., Glagov, S., 1964. Structural basis for the static mechanical properties of the aortic media. *Circ. Res.* 14, 400–413. <https://doi.org/10.1161/01.RES.14.5.400>.
- Wu, P., Nakamura, N., Kimura, T., Nam, K., Fujisato, T., Funamoto, S., Higami, T., Kishida, A., 2015. Decellularized porcine aortic intima-media as a potential cardiovascular biomaterial. *Interact. Cardiovasc. Thorac. Surg.* 21, 189–194. <https://doi.org/10.1093/icvts/ivv113>.
- Wu, J., Zhou, Y., Lemmon, E.W., 2011. An equation of state for the thermodynamic properties of dimethyl ether. *J. Phys. Chem. Ref. Data* 40, <https://doi.org/10.1063/1.3582533> 023104.
- Xing, Q., Yates, K., Tahtinen, M., Shearier, E., Qian, Z., Zhao, F., 2015. Decellularization of fibroblast cell sheets for natural extracellular matrix scaffold preparation. *Tissue Eng. Part C Methods* 21, 77–87. <https://doi.org/10.1089/ten.tec.2013.0666>.
- Xu, H., Xu, B., Yang, Q., Li, X., Ma, X., Xia, Q., Zhang, Y., Zhang, C., Wu, Y., Zhang, Y., 2014. Comparison of decellularization protocols for preparing a decellularized porcine annulus fibrosus scaffold. *PLoS One* 9, e86723. <https://doi.org/10.1371/journal.pone.0086723>.